Biochimica et Biophysica Acta, 728 (1983) 455–459
Elsevier Biomedical Press

BBA Report

BBA 70081

MEMBRANE POTENTIAL PLAYS A DUAL ROLE FOR CHLORIDE TRANSPORT ACROSS TOAD SKIN

ERIK HVIID LARSEN and BJØRN E. RASMUSSEN

Zoophysiological Laboratory A, August Krogh Institute, Universitetsparken 13, DK 2100 Copenhagen Ø (Denmark)

(Received December 13th, 1982)

Key words: Cl^--transport; Potential gating; Two-membrane theory; Hodgkin-Huxley kinetics; Computer model; (Toad skin epithelium)

The Cl^--current through toad skin epithelium depends on the potential in a way consistent with a potential-controlled Cl^- permeability. Computer analysis of the Koefoed-Johnsen Ussing two-membrane model provided with constant membrane permeabilities indicates that the voltage- and time-dependent currents are not caused by a trivial Goldmand-type rectification and ion redistributions following transepithelial potential pertubations. Extended with a dynamic Cl^- permeability in the apical membrane according to a Hodgkin-Huxley kinetic scheme, the model predicts voltage clamp data which closely resemble experimental observations. This extension of the classic frog skin model implies that the Cl^- permeability is activated by a voltage change caused by the inward Na^+ current through the apical membrane.

Gating type models which were introduced by Hodgkin and Huxley [1] have provided the conceptual framework for the quantitative analysis of electrical phenomena in excitable membranes. Our studies suggest that in addition these models furnish a powerful extension to the Koefoed-Johnsen Ussing two-membrane model [2] of NaCl transport in amphibian epithelia. The two-membrane model implies that the potential across the frog skin is due to different permeability properties of outward and inward facing membranes. Whereas the outer membrane is more permeable to Na^+ than to K^+, the inner membrane is more permeable to K^+ than to Na^+. An Na^+, K^+-pump in the inner membrane produces a low intracellular Na^+ concentration, a high intracellular K^+ concentration, and a transcellular inward flux of Na^+. The resulting potential difference (outside of the skin negative) provides the driving force for Cl^- uptake. We report here a dual role for the potential across the toad skin: In addition to the classic view that it is responsible for driving chloride ions through the skin, the potential controls the Cl^- permeability.

Our experiments were carried out with belly skins of the toad (*Bufo bufo*) mounted under voltage clamp conditions [3,4]. Hyperpolarization (outside of the skin more negative than resting potential) leads to a large outward going current associated with an inward flux of Cl^- (Fig. 1a). The steady-state conductance-voltage curve decreases strongly between -70 mV and 0 mV and becomes constant outside these limits. Replacement of Cl^- with SO_4^{2-} in the mucosal bath leads to a V-independent membrane conductance, illustrating the high Cl^--specificity of the rectifying pathway (Fig. 1b, and Ref. 3). The time course of transition between low and high Cl^--conductance is sigmoidal with a half-time ($T_{1/2}$) increasing as a function of clamping potential (Fig. 1c, d). Flux-ratio analysis [5] showed that chloride ions pass the activated pathway by way of simple passive transport [4,6]. These findings point to a potential dependent passive Cl^- permeability. Two more experimental findings favour this interpretation. (a) In the voltage clamp mode the time constant of conductance activation ($T_{1/2}$) is independent of the Cl^- current through the skin [6], and conduc-

0005-2736/83/0000–0000/$03.00

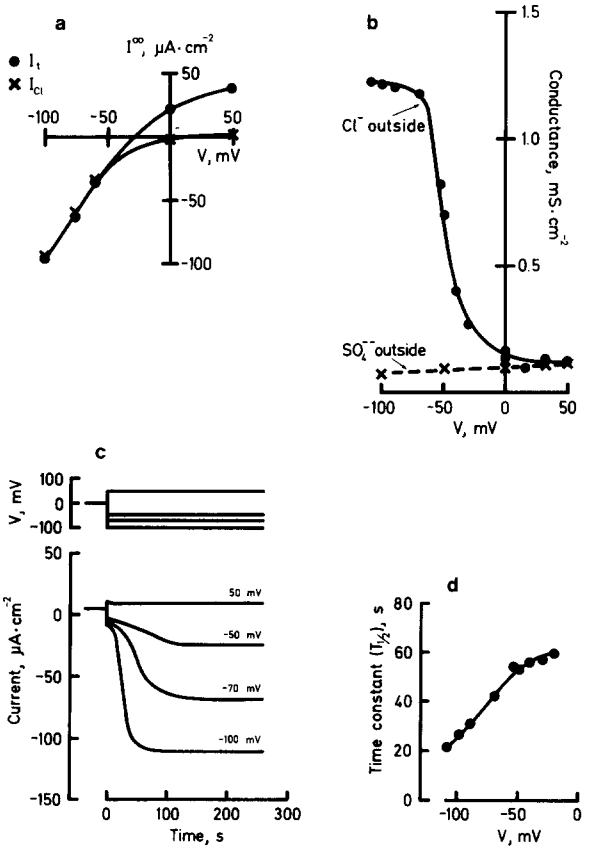

Fig. 1. (a) Voltage dependence of steady-state total current (I_t) and steady-state Cl^- current (I_{Cl}) of toad skin exposed to NaCl-Ringer on serosal and mucosal side (112 mM Na^+, 2.4 mM K^+, 1.0 mM Ca^{2+}, 114 mM Cl^-, 2.4 mM HCO_3^-, pH 8.2). V is the potential of outside solution minus that of inside, inward currents are positive. Measurements of unidirectional fluxes by means of $^{36}Cl^-$ according to Ref. 3. For clarity only the mean values are included in the diagram. The mean values and their standard errors are as follows (in μA·cm^{-2}, $N = 5$ skin preparations); -100 mV: $I_t = -97 \pm 8$, $I_{Cl} = -94 \pm 9$; -75 mV: $I_t = -63 \pm 5$, $I_{Cl} = -59 \pm 7$; -60 mV: $I_t = -38 \pm 2$, $I_{Cl} = -37 \pm 3$; 0 mV: $I_t = 22 \pm 3$, $I_{Cl} = -2.1 \pm 0.9$; $+50$ mV: $I_t = 38 \pm 4$, $I_{Cl} = 1.2 \pm 0.8$. The voltage clamp sequence started at $+50$ mV and proceeded stepwise to -100 mV. The preparations were clamped at 1 h at each clamp potential. Samples for counting of Cl^- activities were taken at 20-min intervals. The first 20-min period at each clamp level was omitted for the calculation of tracer fluxes. (b) Steady-state (slope) conductance-voltage curve of toad skin exposed to NaCl-Ringer on the mucosal side (●), or to a mucosal solution with Cl^- substituted by SO_4^{2-} (×). At each potential the membrane conductance was calculated from the current response to a $+10$ mV voltage pulse of 500 ms duration. (c) Family of clamping currents following a stepwise change of V from zero to the potentials indicated on the records (voltage clamp program on top). (d) V-dependence of the half-time ($T_{1/2}$) of current activation initiated from a holding potential of 0 mV.

tance activation as well as deactivation occur even at zero transepithelial current flow [4]. (b) The temperature coefficient of $1/T_{1/2}$ is larger than that of steady-state Cl^- current ($Q_{10}(1/T_{1/2}) = 1.77 \pm 0.07$, $Q_{10}(I^{\infty}) = 1.14 \pm 0.05$, mean ± S.E. see Ref. 6), both being measured by bringing the membrane from the closed to fully activated state. These values differ significantly ($P < 0.05\%$, $N = 8$).

For a single membrane, results of the above type provide a sufficient basis for proposing that conductance activation and ion translocation are independent processes. Furthermore, it would be justified to assume that conductance activation is due to a potential controlled gating reaction, for example of the type [1,8]:

$$\underset{1-s}{\text{channels closed}} \overset{\alpha}{\underset{\beta}{\rightleftharpoons}} \underset{s}{\text{channels open}}$$

where α and β are potential-dependent rate coefficients, and s gives the fraction of open channels at a given membrane potential and time. However, toad skin epithelium is a multicellular membrane with an intracellular compartment of low Cl^- concentration. Slow current relaxations following voltage clamping of this membrane may originate from intracellular redistribution of ions. A similar idea was advocated by Attwel et al. [9] in their three compartment model of a cardiac muscle preparation, although the ion redistribution was located just outside the cell membrane. In their mathematical treatment they analyzed redistribution of non major ion current carriers between bulk and extracellular cleft compartment. This procedure is not valid for our system in which Cl^- is a major current carrier across the cell boundaries (for discussion, see Refs. 4 and 6). A general mathematical solution based on the two-membrane model of Koefoed-Johnsen and Ussing has been given for the steady state [3,10,11] and recently Lew et al. [12] supplied the non steady-state solution. Common to these treatments and our non steady-state solution of the voltage clamp mode [4,7] is the assumption that passive conductors behave according to the steady-state Nernst-Planck equation integrated through a constant field membrane, and that the kinetics of the inner membrane Na^+,K^+ pump are that of the red cell pump

[13]. Recently, the last mentioned assumption has been verified for the granulosum cells of frog skin [14–16]. In the calculations we assume that the Cl^- current passes through sodium transporting cells. Probably, these are not the granulosum cells. Recent evidence suggest that the transepithelial Cl^- pathway is located to the mitochondria-rich cells [17–19], which also seem to participate in the transepithelial Na^+ transport [20].

Based on potential independent membrane permeabilities our computer model analysis shows that non-linear steady-state current-voltage curves are to be expected. Assuming that the outer membrane Cl^- permeability is larger than its Na^+ permeability, the *I-V* curve is concave towards the *V*-axis with a large Cl^- current at hyperpolarizing potentials as is observed in living tissue (Fig. 2a). However, transient currents of ion redistribution processes relax almost monoexponentially (Fig. 2b). From a holding potential of 0 mV the half-time of these currents decreases as a function of clamping potential (Fig. 2c). This is incompatible with observations on toad skin as well as in excitable membranes. In the skin, following hyperpolarization relaxation currents display an initial delay, and the potential variation of $T_{1/2}$ (Fig. 1d) is opposite to that predicted by the model (Fig. 2c). Therefore, we extended the mathematical treatment of the two-membrane model by incorporating a passive Cl^- permeability (P^o_{Cl}) in the outer membrane gated by the membrane potential (V_o). In analogy with the Hodgkin-Huxley theory [1] we make the following assumptions:

$$P^o_{Cl} = P^o_{Cl}(\max)\, s^n \tag{1}$$

$$ds/dt = \alpha(1-s) - \beta s \tag{2}$$

$$\alpha = f(V_o) \tag{3}$$

$$\beta = h(V_o) \tag{4}$$

where n is a positive integer, and $P^o_{Cl}(\max)$ is the fully activated outer membrane Cl^- permeability.

With this modification, the model predicts voltage clamp behaviour which compares fairly well with that observed for toad skin. The example given in Fig. 3 is for illustrative purposes, and it shows that the agreement holds with respect to

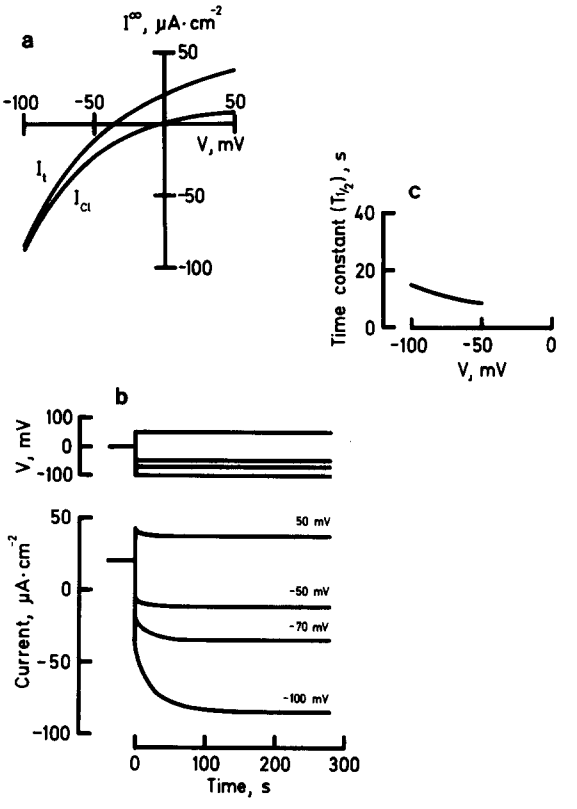

Fig. 2. Computer analysis of the epithelial membrane model with *V*-independent membrane permeabilities. NaCl-Ringer in inside and outside compartments (see legend to Fig. 1). Outer membrane permeabilities (10^{-6} cm·s^{-1}): $P^o_{Na} = 0.5$, $P^o_K = 0.1$, $P^o_{Cl} = 10$. Inner membrane permeabilities (10^{-6} cm·s^{-1}): $P^i_{Na} = 0.01$, $P^i_K = 25$, $P^i_{Cl} = 12$. Paracellular shunt permeabilities (10^{-8} cm·s^{-1}): $P^s_{Na} = 1.7$, $P^s_K = 2.5$, $P^s_{Cl} = 1.0$. Maximum Na^+ flux through inner membrane pump = 0.6 nmol·cm^{-2}·s^{-1}, Na^+-dissociation constant of the pump = 3.4 mM, Na^+-pump flux/K^+-pump flux = 3/2. Inner membrane KCl-reflection coefficient = 0.95, amount of non-diffusible intracellular anions (with a mean charge of -2) = $2.5 \cdot 10^{-8}$ mol·cm^{-2}, corresponding to a cell water volume of approx. 340 nl·cm^{-2}. (a) *V*-dependence of steady-state total current (I_t) and Cl^- current (I_{Cl}). The computed short-circuit current (19.9 μA·cm^{-2}) and intracellular concentrations of Na^+ (8.2 mM), K^+ (143.4 mM), and outer membrane potential (91.9 mV, mucosa positive), and transcellular voltage divider ratio of 0.74 at short-circuit conditions approximate well values measured in the granulosum cells of amphibian skin, whereas the computed intracellular Cl^- concentration (3.1 mM) is significantly lower [15,20–22]. The relevance of these comparisons may be questioned, however, as the mitochondria-rich cells are the candidates of transcellular Cl^- current flow [17–19]. (b) Computed time-dependence of accumulation/depletion currents of the model epithelium. Voltage clamp program on top. (c) *V*-dependence of $T_{1/2}$ of the current transients shown in Fig. 2b (holding potential 0 mV).

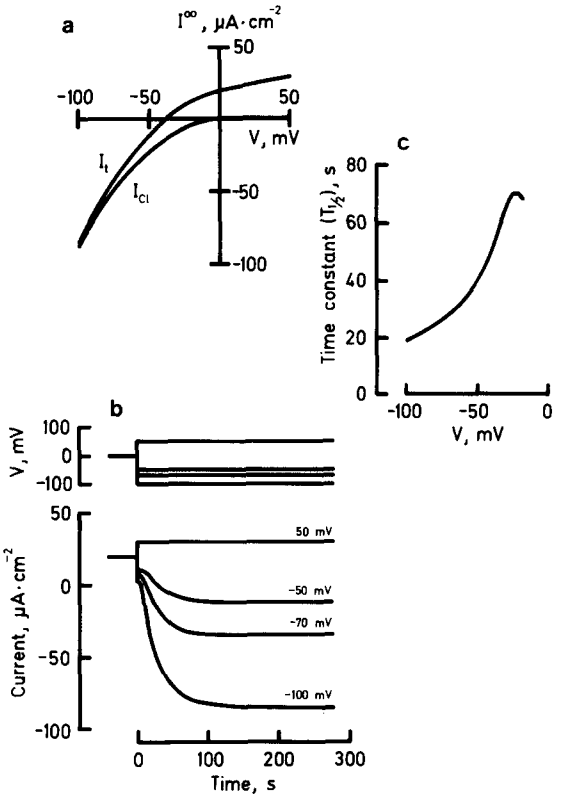

Fig. 3. Computer analysis of the epithelial membrane model extended with a V-dependent outer membrane Cl^- permeability according to (see Eqns. 1, 3 and 4 in the text)

$$P_{Cl}^{o} = 10^{-5} s^{6} \qquad (1a)$$

$$\alpha = 0.0014(V_o - 85)/(\exp((V_o - 85)/12) - 1) \qquad (3a)$$

$$\beta = 0.06/(\exp(-(V_o - 80)/3) + 1) \qquad (4a)$$

where V_o is the outer membrane potential in mV (potential in mucosal solution minus that in cell), and α and β are in units of s^{-1}. All other independent variables are given in legend to Fig. 2. (a) Computed steady-state total current (I_t) and Cl^- current (I_{Cl})-voltage curves. (b) Computed time course of voltage clamp currents. The same voltage clamp program (given on top) was applied at the computer terminal and in the laboratory (see Fig. 1c). (c) $T_{1/2}$ of the non steady-state voltage clamp currents shown in Fig. 3b (holding potential 0 mV).

shape of I-V graphs, steady-state currents, shape of current-time curves, and time scale (compare diagrams a, c and d of Fig. 1 and Fig. 3). The computed current-time curves shown in Fig. 3b are predominantly gated currents but contain accumulation/depletion components, as well. For example, activation at $V = -100$ mV, the numerical solution predicts an increase of P_{Cl}^{o} from $3.7 \cdot 10^{-10}$ cm·s^{-1} to $1.0 \cdot 10^{-5}$ cm·s^{-1}, and the following changes in intracellular concentrations of Na^+, K^+ and Cl^- (mM): -5.2, 0.5, and 17.8 from their steady-state values at short-circuit conditions (mM): 8.2, 143.4, and 3.1, respectively, and a cell water volume change from 337 to 397 nl·cm^{-2}. Since the outer membrane resistance decreases with activation, V_o and thereby α and β vary with time (for $V = -100$ mV, computed instantaneous and steady-state values of V_o are -0.9 mV and 0.7 mV, respectively, but V_o varies non-monotoneously with time achieving a maximum value of 15.1 mV after 20 s). In view of this high degree of complexity in the kinetics of slow voltage clamp currents, the above set of equations governing uptake of Cl^- across the apical membrane is only

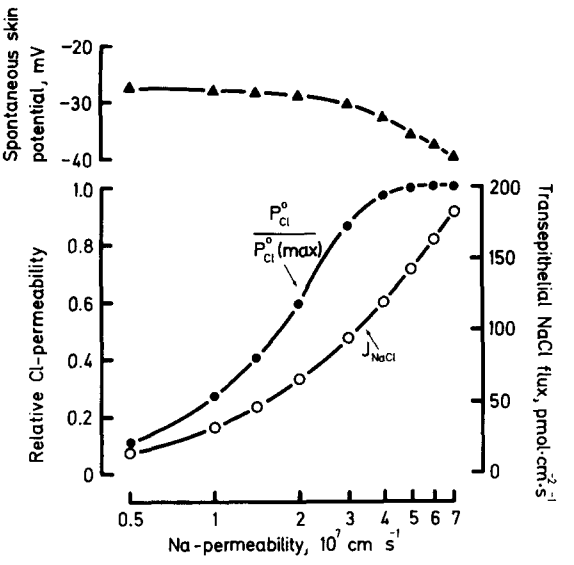

Fig. 4. Computer analysis of the epithelial membrane model extended with a potential-dependent Cl^- permeability (see legend to Fig. 3). Open circuit state (zero transepithelial current). The model predicts strong dependence of outer membrane Cl^- permeability (here depicted relative to its maximum value) on outer membrane Na^+ permeability (P_{Na}^{o}). J_{NaCl} is the computed transepithelial (inward) flux of NaCl. The transepithelial potential varies from -27.6 mV ($P_{Na}^{o} = 0.5 \cdot 10^{-7}$ cm·s^{-1}) to -39.8 mV ($P_{Na}^{o} = 7 \cdot 10^{-7}$ cm·s^{-1}), corresponding to a variation of the outer membrane potential from +75.4 mV to 52.5 mV (mucosal solution positive). Since the mathematical description of the voltage dependence of the outer membrane Cl^- permeability is approximative, the above graphs reveal the quality of relationships, only.

an approximation. This is also evident from the fact that the initial delay of current activation at $V = -100$ mV is not fully accounted for by raising the gating variable to the power of 6.

The hypothesis that membrane potential controls chloride permeability means that under open circuit conditions the Na^+ current through the outer membrane sets the Cl^- permeability of the skin. To illustrate this we have solved the system of equations numerically for different Na^+-permeabilities (P^o_{Na}) corresponding to measured values in non-stimulated and hormonal stimulated preparations [23–25]. Fig. 4 shows that our theory predicts a 10-fold variation of Cl^- permeability within the physiological range of Na^+ permeabilities. According to the model (Fig. 4), the large increase in NaCl uptake with P^o_{Na} stimulation is accompanied by a minor increase in transepithelial potential difference (less than 15 mV), thus leaving the paracellular leakage fluxes almost unaffected. From this dependence of Cl^- uptake on Na^+ current, it is to be expected that unidirectional Cl^- fluxes in the short-circuited skin decrease following removal of mucosal Na^+ or by blocking the Na^+ permeability with amiloride, which has been found in experiments with frog skin [26–28].

This study was supported by the Danish Natural Science Research Council grants 511-7120, 11-0583 and by the NOVO Foundation.

References

1 Hodgkin, A.L. and Huxley, A.F. (1952) J. Physiol. (London) 117, 500–544
2 Koefoed-Johnsen, V. and Ussing, H.H. (1958) Acta Physiol. Scand. 42, 298–308
3 Larsen, E.H. and Kristensen, P. (1978) Acta Physiol. Scand. 102, 1–21
4 Larsen, E.H. and Rasmussen, B.E. (1982) Phil. Trans. Roy. Soc. Lond. B. 299, 413–434
5 Ussing, H.H. (1949) Acta Physiol. Scand. 19, 43–56
6 Larsen, E.H. (1982) in Chloride Transport in Biological Membrane (Zadunaisky, J., ed.), pp. 333–364, Academic Press, New York
7 Larsen, E.H., Rasmussen, B.E. and Willumsen, N. (1981) Adv. Physiol. Sci. 3, 115–127
8 Jack, J.J.B., Noble, D. and Tsien, R.W. (1975) Electric Current Flow in Excitable Cells, Clarendon Press, Oxford
9 Attwell, D., Eisner, D. and Cohen, I. (1979) Q. Rev. Biophys. 12, 213–261
10 Lindemann, B. (1977) Bioelectrochem. Bioenerg. 4, 275–286
11 Lindemann, B. (1977) Bioelectrochem. Bioenerg. 4, 287–297
12 Lew, V.L., Ferreira, H.G. and Moura, T. (1979) Proc. R. Soc. Lond. B 206, 53–83
13 Garay, R.P. and Garrahan, P.J. (1973) J. Physiol. (London) 231, 297–325
14 Larsen, E.H., Fuchs, W. and Lindemann, B. (1978) Eur. J. Physiol. S82, R13
15 Nielsen, R. (1982) J. Membrane Biol. 65, 221–226
16 Nagel, W. (1980) J. Physiol. (London) 302, 281–295
17 Voûte, C.L. and Meier, W. (1978) J. Membrane Biol. 40S, 154–165
18 Kristensen, P. (1981) Acta Scand. Physiol. 113, 123–124
19 Ussing, H.H. (1982) in Functional Regulation at the Cellular and Molecular Levels (Corradino, R.A., ed.), pp. 285–297, Elsevier/North-Holland, Amsterdam
20 Rick, R., Dörge, A., Von Arnim, E. and Thurau, K. (1978) J. Membrane Biol. 39, 313–331
21 Nagel, W., Garcia-Diaz, J.C. and Armstrong, W.McD. (1981) J. Membrane Biol. 61, 127–134
22 Helman, S.I. and Fischer, R.S. (1977) J. Gen. Physiol. 69, 571–604
23 Fuchs, W., Larsen, E.H. and Lindemann, B. (1977) J. Physiol. (London) 267, 137–166
24 Li, J.H.-Y., Palmer, L.G., Edelman, I.S. and Lindemann, B. (1982) J. Membrane Biol. 64, 77–89
25 Palmer, L.G., Li, J.H.-Y., Lindemann, B. and Edelman, I.S. (1982) J. Membrane Biol. 64, 91–102
26 Candia, O.A. (1978) Am. J. Physiol. 234, F437–F445
27 Kristensen, P. (1978) J. Membrane Biol. 40S, 167–185
28 Rotunno, C.A., Ques-Von Petery, M.V. and Cereijido, M. (1978) J. Membrane Biol. 42, 331–343